Enantiomer-selective molecular sensing using racemic nanoplasmonic arrays

Jose García-Guirado[1], Mikael Svedendahl[1,2], Joaquim Puigdollers[3], Romain Quidant[1,4,*].*

1-ICFO-Institut de Ciencies Fotoniques, The Barcelona Institute of Science and Technology, 08860 Castelldefels (Barcelona), Spain.

2-KTH Royal Institute of Technology, Roslagstullsbacken 21, 10691 Stockholm, Sweden.

3-Universitat Politècnica de Catalunya (UPC), Departament d'Ingeniería Electrónica, 08034 Barcelona, Spain.

4-ICREA-Institució Catalana de Recerca I Estudis Avançats, 08010 Barcelona, Spain.

KEYWORDS: Biosensing, chiral sensing, plasmonics, optical chirality, enantiomers.

Building blocks of life show well-defined chiral symmetry which has a direct influence on their properties and role in Nature. Chiral molecules are typically characterized by optical techniques such as circular dichroism (CD) where they exhibit signatures in the ultraviolet frequency region. Plasmonic nanostructures have the potential to enhance the sensitivity of chiral detection and translate the molecular chirality to the visible spectral range. Despite recent progress, to date, it remains unclear which properties plasmonic sensors should

exhibit to maximize this effect and apply it to reliable enantiomer discrimination. Here, we bring further insight into this complex problem and present a chiral plasmonic sensor composed of a racemic mixture of gammadions with no intrinsic CD, but high optical chirality and electric field enhancements in the near-fields. Owing to its unique set of properties, this configuration enables us to directly differentiate Phenylalanine enantiomers in the visible frequency range.

Chirality, geometrically understood as the lack of symmetry under specular reflection, is of major importance in biological systems as well as biological and chemical processes.[1,2] For example, biological receptors for taste and smell are sensitive to enantiomers, the two mirrored images of a chiral molecule, and can chemically differentiate them by producing different responses that we interpret as, for instance, drastically different scents.[3,4] This asymmetry is critical in the case of the physiological action of drugs, where in the worse scenario one enantiomer acts as a medicine while the other has detrimental effects.[5,6]

Since such critical biological actions can be related with chirality, several spectroscopic techniques have been developed over the years to differentiate enantiomers. Such techniques include circular dichroism (CD), optical rotatory dispersion (ORD) and Raman optical activity (ROA).[7,8] Although powerful, these techniques suffer from low signals and sensitivity (ROA) or are located in UV spectral range (CD and ORD), which rely on expensive equipment.[9] It should be noted that the chiro-optical response of biomolecules is generally weak, thus high concentrations and analyte volumes are required.

The recent developments in nanotechnology come with novel metamaterials and nanophotonic sensors that exhibit high sensitivity and promising properties for bio-sensing applications.[10–12] These sensors concentrate light efficiently, creating highly sensitive nano-regions that interact strongly with matter and can be used to detect very small amounts of molecules through changes in their optical response.[13–16] Nanostructures and metamaterials can also be designed to mimic the properties of chiral molecules, controlling the polarization of light in a given wavelength range.[17–25] For instance, giant circular dichroism signals have been reported in the visible (VIS) and near infra-red (NIR) spectral range.[19,25] Additionally, nanostructures can be devised to provide local fields with large so-called optical chirality, *C,* defined as $C = \frac{-\varepsilon_0}{2\omega} Im(\bar{E}^* \cdot \bar{B})$. Here, ε_0 is the vacuum permittivity, ω the angular frequency of light, and $\bar{E}$ and $\bar{B}$ are the electric and magnetic fields of light, respectively. Considering that C is ±1 for left (σ^+) and right (σ^-) circularly polarized light respectively, larger values may promote stronger light-molecule interactions and thus be beneficial for the detection of chiral molecules.[26–29] However, there can also be a strong interaction between localized plasmons in metallic nanostructures and chiral molecules that induce CD signals through dipole and multipole Coulomb interactions.[30–32] Although it is still not clear what is the best way to extract conformational information from molecular signals coupled to plasmonic systems, several methods have been proposed for the detection of chiral molecules.[30,33–37] While most of these methods use CD as a primary measurement of chirality, some works have also used related signals, e.g. differential transmission, and proposed different ways of extracting the chiral information from the molecules.[37–39] There are several reports on induced CD from molecules near non-chiral plasmonic structures, that is, structures that exhibit no intrinsic CD signals.[31,40–42] This method generally relies on plasmonic systems with high electric fields enhancements, but low *C*.

Recently, attention has turned towards chiral plasmonic array-based sensors that experience both large intrinsic CD and *C*.[38,39] However, the drawbacks of these designs has been (1) the high intrinsic CD of the sensors (Fig. 1a-b), often orders of magnitude bigger than molecules, that potentially could over-shadow the small molecular signals and (2) the need for multiple measurements on separate left- and right handed sensors.[38,39,43]

In this work, we propose a plasmonic sensor (Fig 1c) with highly chiral individual components arranged in a 2D arrangement together with the enantiomeric counterpart, which result in a non-chiral superstructure. This sensor design has important advantages in terms of both functionality and reliability. While using chiral sensors is desired to achieve high optical chirality, the strong far field CD from the sensors ends up masking the much weaker molecular response. This requires post processing the data in order to extract the chiral signature from the molecules, which eventually can be a source of severe artefacts. Indeed, the subtraction of two very similar spectra may not be reliable especially when involving nano-sensor array that are not fully identical due to nanofabrication deviations. Eventually, our measurements give a direct chiral signature from the molecules hence dramatically increasing the reliability of the sensor. As illustrated in Fig. 1, such a racemic mixture of chiral sensors can keep as large values of C and electric field enhancements in the near fields as the totally handed sensors and at the same time the CD signal of the sensor is suppressed. Racemic sensor arrays have recently been suggested for chiral molecular detection,[43] however this detection scheme has not been implemented experimentally until now. The main idea behind such a sensor is that one molecular enantiomer will interact more with one sensor component, which will shift the CD balance of the entire sensor system and yield a detectable signal. The CD signal is anticipated to mainly depend on the CD and *C* factor of the sensor components, as the main absorption and CD resonances of chiral

molecules reside in the UV. We show that the racemic sensor can be used for direct molecular detection and discrimination between the two phenylalanine enantiomers. D, L and the racemic forms (i.e. D+L at 50/50 concentration, denoted as DL) of the amino-acid are used in order to validate and link the results unambiguously to the chiral conformation of the molecules.

Beyond the use of racemic sensors, another novelty of our study over the prior art is the way the molecules are controllably delivered to the sensors using molecular thermal evaporation (MTE),[44] a rarely used method in this field, but extensively used in molecular electronics. Molecular delivery has also been a limitation in past studies due to poor control and reproducibility issues. MTE is very suitable for our purpose, since it allows accurate control of the molecular deposit conditions and thickness of the coatings, providing more reproducible, homogeneous and dense molecular layers using a solvent-free method.[45,46]

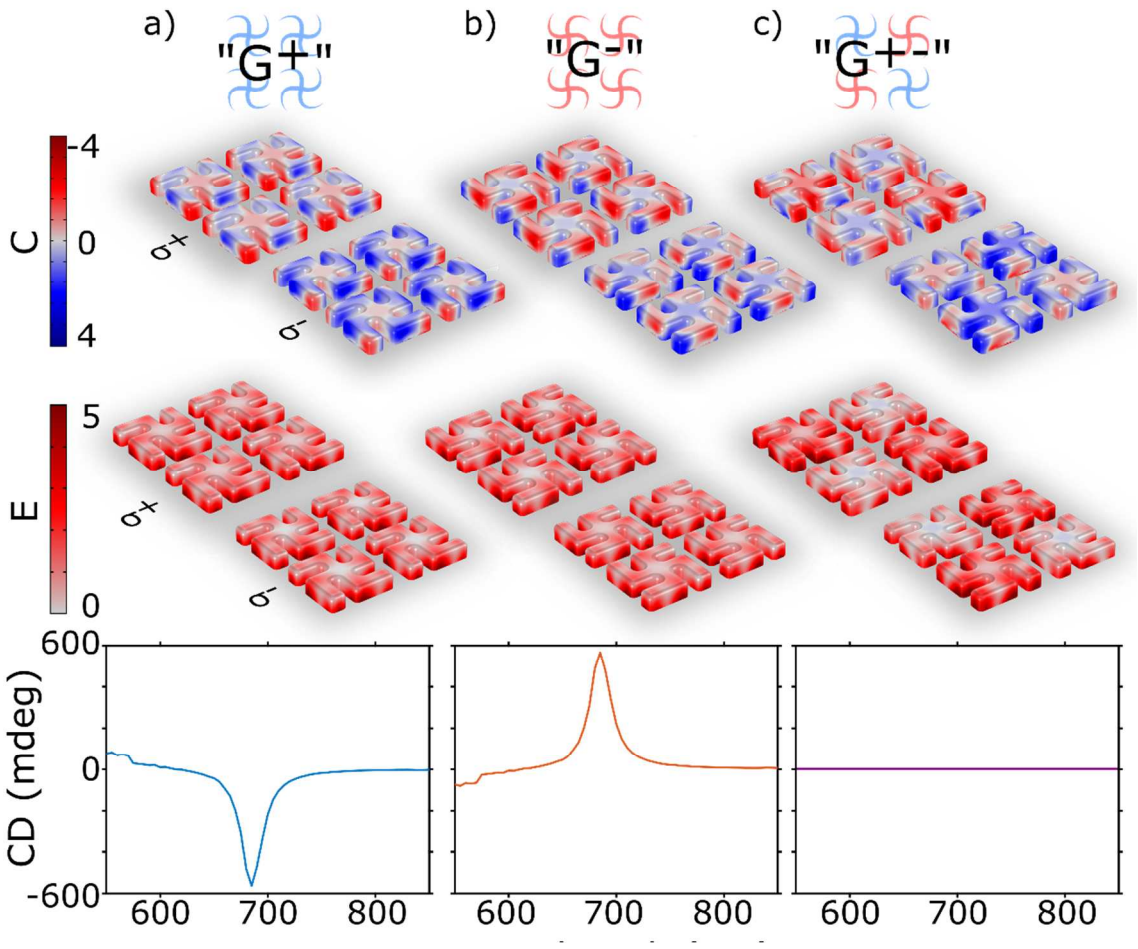

Figure 1: Handed vs. racemic gammadion arrays. The handed arrays, a) G^+ and b) G^-, exhibit large optical chirality (top) and large electric field enhancement (middle), but also large CD (bottom). c) The racemic gammadion array G^{+-} shows large optical chirality and electric field enhancement, but no CD. σ^+ and σ^- indicates excitation with left and right circularly polarized light, respectively.

Racemic plasmonic sensors. Gold chiral plasmonic nano-structures consist of gammadion elements arranged in a 2D matrix array of 120 μm in size. The arrays were produced by electron beam lithography (CRESTEC CABL9510C) using a negative resist (ARN7500.08) on 50 nm

gold coated borosilicate substrates separated by a thin (~2 nm) Ti adhesion layer. After exposure and development, the gold layer was exposed to reactive ion etching (Oxford Plasmalab System 100) followed by resist removal in piranha solution (Caution: piranha solution is a very reactive solution and should be handled with the maximum safety precaution). The nano-structures were optically characterized using a custom-made setup consisting of a white light source (100w halogen bulb) followed by a broadband linear polarizer (Thorlabs GL10) and quarter wave plate (Thorlabs FR600QM), then the sample followed by a low numerical objective (Olympus LMPLFLN5x) which couples to a grating spectrometer (Andor Shamrock 303i iDus401-BR-DD system) through an optical fiber. The interrogated area of the sensor is 60 μm in diameter, which account for an averaging over 28,000 gammadion structures.

In order to visualize the properties of racemic gammadion arrays, we compare these with completely handed arrays. Note that both the gammadion structure as well as the racemic and the completely handed arrays have C4 symmetry, which ensures anisotropy-artifact-free measurements.[20] Figure 2 displays scanning electron microscope (SEM, FEI Inspect F) images and spectra of gammadions of 275 nm in size arranged in a 350 nm pitch squared matrix. Here, extinction is defined as $E = 1 - T$, where T is the transmitted light, and the CD is calculated using

$$CD = atan\left(\frac{\sqrt{T_{\sigma^-}} - \sqrt{T_{\sigma^+}}}{\sqrt{T_{\sigma^-}} + \sqrt{T_{\sigma^+}}}\right),$$

where T_{σ^+} and T_{σ^-} is the transmission of left and right circularly polarized light, respectively. The handed arrays had extinction and CD resonances at 660 nm, either in their G^+ or G^- form, as indicated in Fig. 2. For the racemic mixture, G^{+-}, we placed right and left-handed gammadions

alternatively in a row and then shifted the next rows by one. The racemic array showed a flat resonance peak in between 625-675 nm and zero CD signal all over the measured spectral range (Figure 2c). The difference in extinction spectrum is not surprising, as the local environment surrounding a specific gammadion is changed and is thus attributed to the interaction between G^+ and G^- components. This result confirms that, like in molecular systems, right and left enantiomer's *CD* cancel out in a racemic mixture.

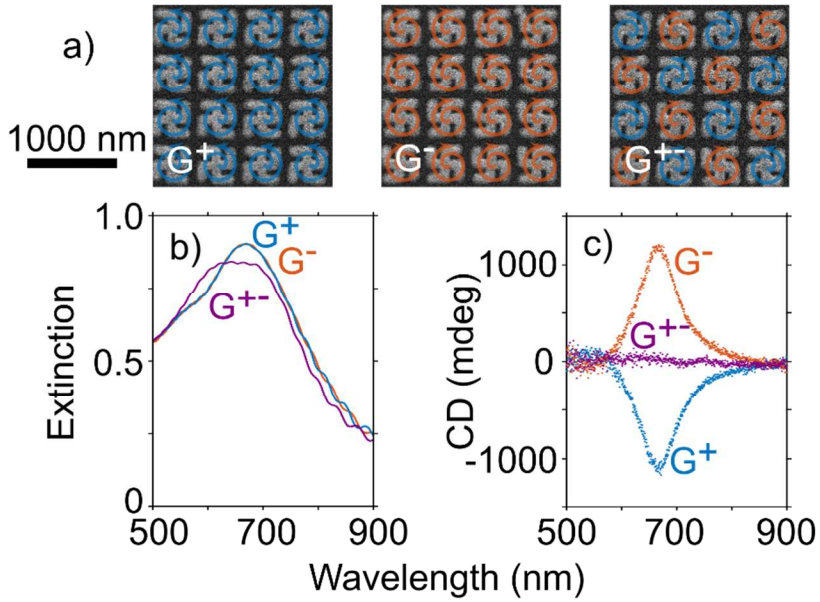

Figure 2: Optical characterization of handed and racemic gammadion arrays. a) SEM images of handed G^+ and G^- arrays, as well as the racemic G^{+-} array. b) Extinction and c) CD spectra of the fabricated nanostructures.

Molecular layers. Mostly, previous works not only use different sensor systems, but also different chiral molecules like polymeric chains or proteins.[31,38,40] These large molecules can possess supra-structural CD, which might be easier to detect, but the mirror molecule is seldom

available, which makes the results difficult to validate thoroughly. On the other hand, enantiomeric systems are typically small and therefore produce small signals that are more challenging to detect. An ideal sensor should not only be able to detect a chiral molecule, but also give signals which reveal the enantiomer handedness in the sample. To fully validate a sensor, it is thus important to test the full set of molecules: not only the two enantiomers, but also the racemic mixture of the two. Phenylalanine, an essential amino-acid, was chosen in this experiment as both enantiomers and the racemic mixture are commercially available (78019, P1751 & 147966 Sigma Aldrich). Here, we used molecular thermal evaporation (MTE) in order to accurately control the delivery of molecules and ensure a high density coating. In this technique, the molecules sublimate from a crucible and reach the target substrate similarly to what would happen with conventional metal thermal evaporation (Fig 3a). This way, the molecules can reach the interparticle regions and the gaps within the gammadion nanostructures. The thickness of the layers can be carefully adjusted using a quartz crystal microbalance (QCM). First, we deposited the different enantiomers and racemic mixture on a quartz substrate. Phenylalanine molecules were sublimated at 100 °C with a deposition rate of 5 Å/s, leading to an amorphous layer. The thickness was estimated using the QCM readings together with scanning electron microscope images (SEM, Fig. 3b) and was set to be 150 nm in order to fully cover all sensitive areas of the nano-structures. The SEM image confirms the uniformity and thickness of the coating.

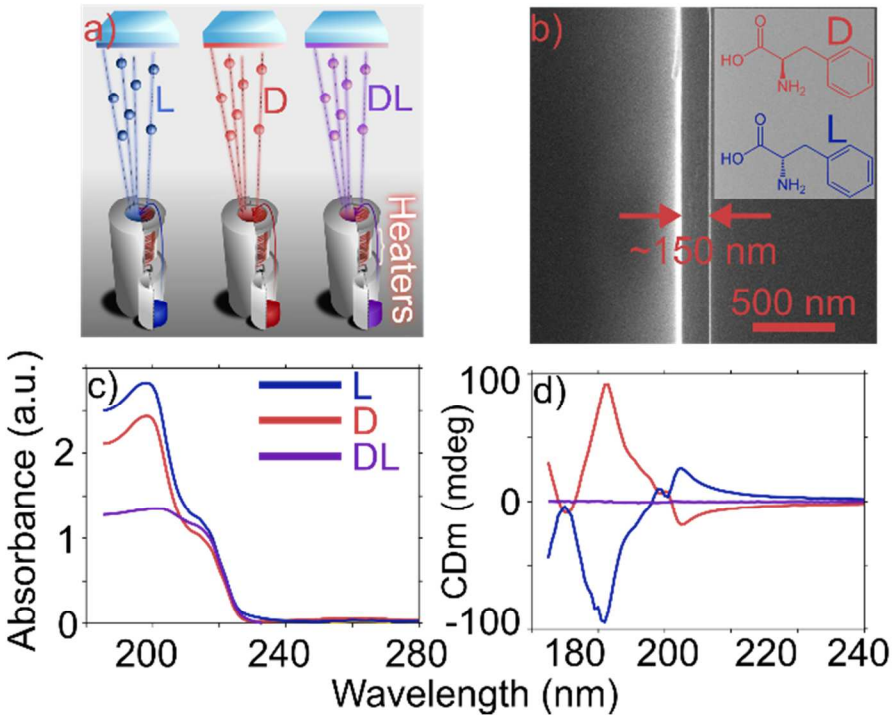

Figure 3: L, D and DL (racemic) coatings of phenylalanine on quartz. a) Schematic of the molecular thermal evaporation technique, where crucibles are filled with the molecules and gently heated under vacuum, until they sublimate and are deposited onto the substrates. b) SEM image of a 150 nm thin layer of DL phenylalanine. c) Absorbance and d) CD spectra of the respective coatings, named CDm to be distinguished from sensors CD.

We then characterized the layers optically in a CD-spectrometer (Applied photo-physics Chirascan plus), as seen in Fig. 3c-d. Absorbance spectra of the coatings reveal a main peak at 200 nm within accordance of 10% for both enantiomers and reflection symmetry of CD. Interestingly, the absorbance of DL coating got a flat peak in a similar fashion as the racemic plasmonic array. As expected, the CD of the racemic mixture is negligible over the entire measurement range, confirming the racemic nature of the mixture film. Note that no CD was measured outside of the displayed spectral range for any of the coatings.

Results. After the previous calibration step on the deposition of molecular layers, we performed evaporations of the different molecules on the racemic plasmonic arrays (Figure 4). The optical measurements were performed in a custom-made setup, which features a detection area four orders of magnitude smaller than the commercial equipment and no lock-in amplification (see Supporting Information for details). Figure 4b-c shows the extinction and CD of the coated plasmonic nano-structures. The flat extinction peak from the bare arrays (Fig 2b) has now become two close, but distinguishable, peaks. Overall, the extinction increased by 20% in height and shifted about 75 nm due to the coatings. Exclusively, DL coating extinction increased an extra 10% and split significantly the two peaks in comparison with D and L coatings extinctions. Even more interestingly, the molecular enantiomers induced CD signals with opposite sign originating from the symmetric molecular system (phenylalanine D and L), about 500 nm from the previous CD peak wavelength. This is made possible thanks to the synergetic effect of the local optical chirality and field enhancement of the sensors which selectively enhances the residual CD of the enantiomers in the VIS-NIR range. Eventually, the signal stems from an unbalance in the racemic array components, in which either G+ or G- interacts more with the interrogated molecules.. In addition, the DL coating induced no significant CD, in line with the CD measurements of the molecular coatings. These results are in accordance with the symmetry of the system, as we already saw in the molecular coatings and in the plasmonic nano-structures. However, a degradation of the signals and symmetry could be expected due to accumulations of experimental errors for the final measurement. The non-zero CD of the racemic coating could thus originate from slight imperfections in fabrication that lead to different CD enhancements together with minor differences in the coating properties (see more details on symmetry observations in the Supporting Information). Additional sets of experiments have successfully

reproduced the results, both in the same as well in a completely new batch of sensors (see Supporting Information).

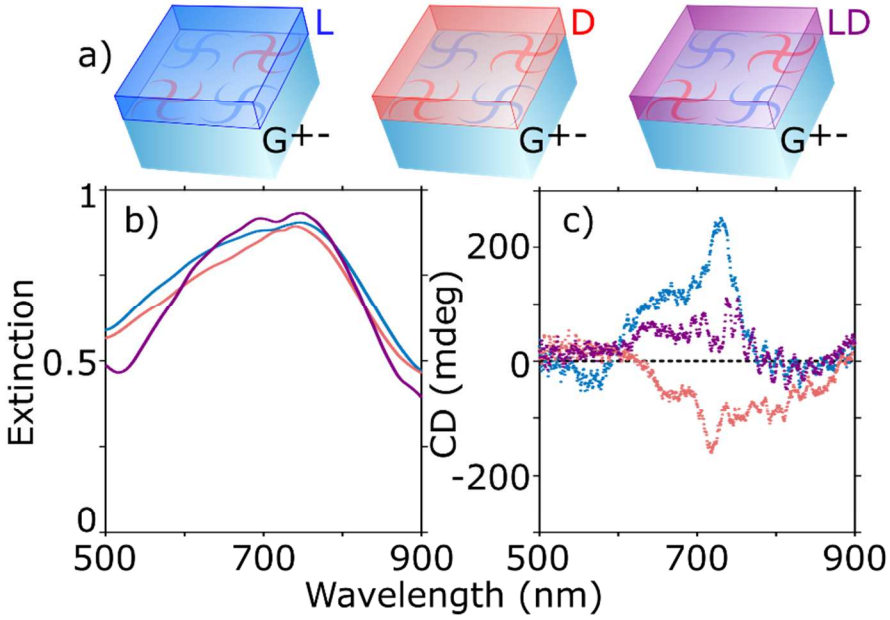

Figure 4: Enantiomer detection in the visible spectral range using racemic gammadion arrays. a) The molecules were deposited on different sensor arrays, showing the corresponding b) extinction and c) CD spectrum.

COMSOL simulations were performed for racemic gammadion arrays on glass (n = 1.5) in molecular refractive index $n_a = 1.6$, using the geometry in Fig. 2 (see Supporting Information for details). Figure 5a-b depicts the results, which show two clear peaks in the extinction spectrum and zero CD, in accordance with the experimental results. Experimental peaks are likely broader due to nano-particle fabrication defects that result in inhomogeneously broadened spectra. Note also that the simulations indicate that while the individual components of the array experience

very large CD but due to the involved symmetry, when combined, the total CD for the array is zero. Consequently, small shifts in this balance could lead to detectable CD signals.

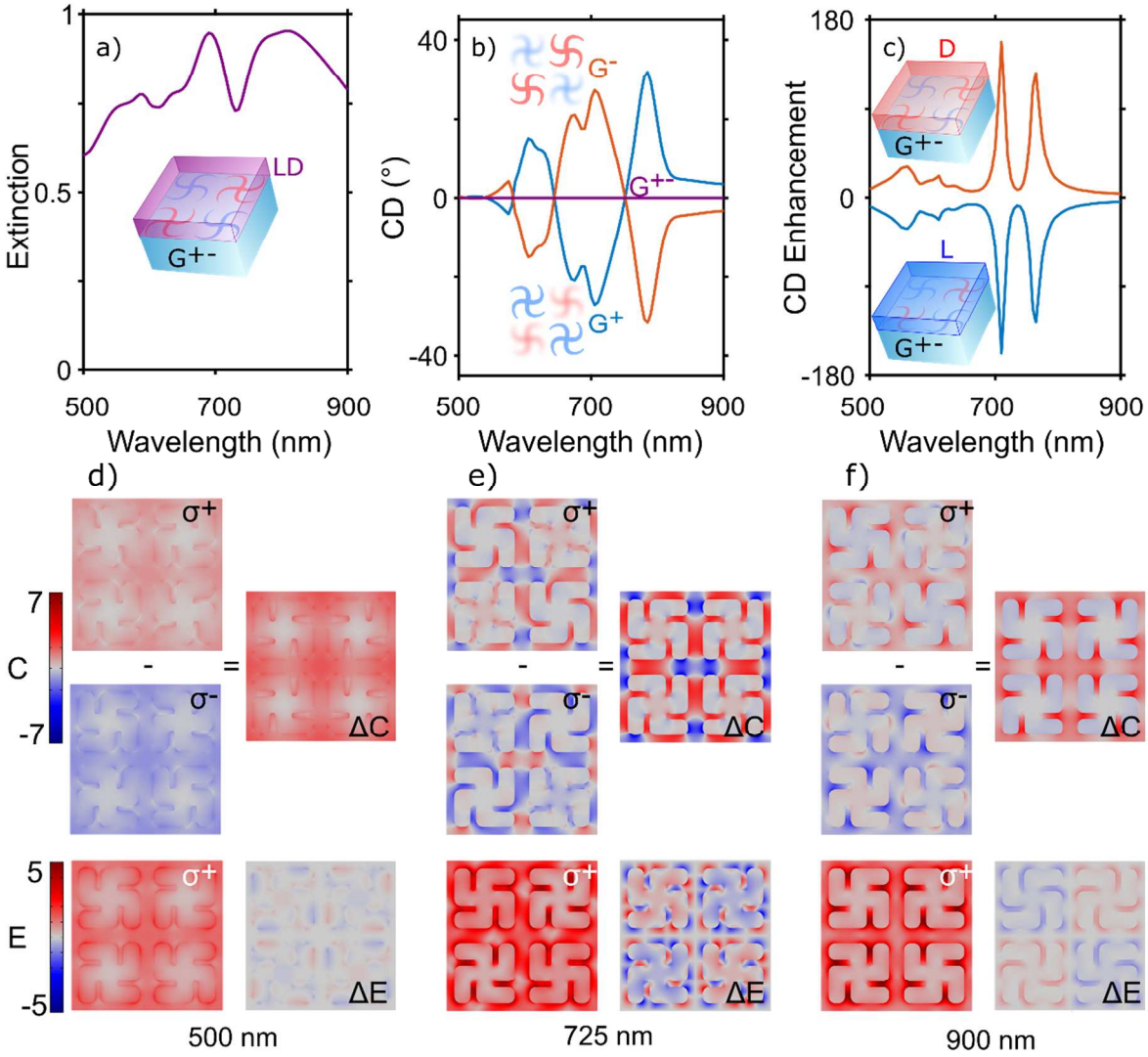

Figure 5: Simulations of gammadions for chiral sensing. a) Extinction and absorption spectra for gammadions on a glass substrate (n = 1.5) and in a n = 1.6 layer with geometries from the SEM in Fig. 2. b) CD spectrum of the individual components of the array (G^+ and G^-), showing large and symmetric CD, and the total CD of the system (G^{+-}), without any CD. c) CD enhancement spectrum for the same array with D and L molecular layers. Optical chirality C, the optical

chirality dissymmetry ΔC, electric field enhancement E and chiral dissymmetry of the electric field enhancement ΔE at d) 500 nm, e) 725 nm and f) 900 nm.

Figure 5c show the CD enhancement spectra of L and D molecules on top of the racemic sensor. The CD enhancement was calculated from the ratio CD_G/CD_0, where CD_G is the CD of the racemic sensor and the chiral layer, while CD_0 is the CD of only the chiral layer without any nanostructures. The over-all line-shape of the simulated spectrum agrees fairly well with the experimental results, even though the latter do not resolve the double peak and feature weaker CD enhancements (see Fig. S4 from Supporting Information). The maximum CD enhancement values are around two orders of magnitude, however, this is likely under-estimated, as the majority of the CD signal originates from a thin layer near the metal, which suggest that it can be much higher locally. In particular, the volume contained between gammadion arms is responsible for about 40% of the CD enhancement (see Fig. S6 from Supporting Information).

Figures 5d-f show C and the E-field enhancement for σ^+ illumination at 500, 725 and 900 nm, together with their chiral dissymmetry, calculated as $\Delta C = C(\sigma^+) - C(\sigma^-)$ and $\Delta E = E(\sigma^+) - E(\sigma^-)$. Due to the racemic composition of the array, reciprocal patterns of C and E are generated using σ^+ and σ^- illumination. Consistent with the experimental results, the strongest C and the E-field enhancement are found at 725 nm. Similarly, ΔC and ΔE are shown to be larger at this wavelength. For a given illumination, the corresponding gammadion within the unit cell, i.e. G^+ under σ^+ or G^- under σ^-, shows stronger E-field enhancement. However, C showed to be larger at odd gammadion-illumination combinations, which is most clearly visualized in the gaps in between the gammadion arms. Regarding C and E dissymmetry, ΔE exhibit clear reflection

symmetry with the gammadion handedness, whereas ΔC exhibit handedness-independent distribution.

Aside from the clear wavelength dependence of these parameters from Fig. 5, the influence of the parameters on the molecule-sensor system is subtler. The sign of C promotes the interaction for a given enantiomer with the sensor. While the magnitude of ΔC shows the difference of this interaction, which would be related to the discrimination capacity of the system and is shown to be independent to the gammadion handedness. On the other hand, E shows the excitation enhancement for a given illumination. For example, G^+ shows a stronger enhancement for σ^+ illumination and, reciprocally, G^- is best excited using σ^-. Hence, ΔE shows the local chiral dependence of the enhancement. Combining these properties of C and E, a given sensor enantiomorph will interact more with a given molecular enantiomer, for example promoting G^+ and L molecule or G^- and D molecule interaction. At the same time, the symmetry of the array yield equal interaction capabilities with both molecular enantiomers. The racemic array thus enables the enantiomer discrimination in a one-shot measurement.

Conclusions. In this study, we measured CD of L, D and racemic phenylalanine on chiral gold nano-structures mixed in an array in a racemic fashion. The designed sensors showed zero intrinsic CD, but locally high optical chirality and electric field enhancements. When in contact with a chiral molecular layer, the CD signal separates from zero, indicating the handedness of the enantiomer near the plasmonic resonance region. This way we demonstrate that plasmonic sensors can be engineered to offer chiral selectivity while they remain intrinsically CD free.

We show that the use of molecular enantiomers, as well the use of racemic molecular mixture as a control, is a key point to confirm chiral detection in plasmonic sensing experiments, which offers a robust model to validate any chiral sensing platform.

Furthermore, phenylalanine species were evaporated using molecular thermal evaporation, a robust deposition technique that allowed us to deposit layers of ~150 nm of the different enantiomers and racemic mixture of the molecules. We believe that this method is an important step forward towards more reproducibility in the loading of the chiral sensors as well as a way to better understand the physical and chemical mechanisms involved in plasmon-enhanced chiral sensing.

ASOCIATED CONTENT

Supporting Information. Supporting material including fabrication, measurement details, and additional sets of data probing experimental repeatability, besides simulation details and a note on the local sensitivity of the structures are included in the document. This material is available free of charge via the Internet at http://pubs.acs.org.

AUTHOR INFORMATION

Corresponding Author. *romain.quidant@icfo.eu, *svedend@kth.se

Notes

The authors declare no competing financial interest.

Author Contributions. J.G., M.S. and R.Q. conceived the project. J.G. designed and built the optical setup, developed the acquisition software, carried out sample fabrication and performed the measurements. J.P. performed the molecular coatings. M.S. performed the COMSOL simulations. J.G., M.S. and R.Q. wrote the manuscript. All authors read and commented on the manuscript.

ACKNOWLEDGMENT

The authors acknowledge financial support from the European Community's Seventh Framework Program under grant QnanoMECA (64790), Fundació Privada Cellex, the CERCA programme and the Spanish Ministry of Economy and Competitiveness, through the "Severo Ochoa" Programme for Centres of Excellence in R&D (SEV-2015-0522) and grant FIS2016-80293-R, the Swedish Research Council (637-2014-6894), and B. Braun Surgical S.A.

REFERENCES

(1) Brandt, J. R.; Salerno, F.; Fuchter, M. J. The Added Value of Small-Molecule Chirality in Technological Applications. *Nat. Rev. Chem.* **2017**, *1* (6), 0045.

(2) Barron, L. D. *Molecular Light Scattering and Optical Activity*; Cambridge University Press: Cambridge, 2004.

(3) Leitereg, T. J.; Guadagni, D. G.; Harris, J.; Mon, T. R.; Teranishi, R. Chemical and Sensory Data Supporting the Difference between the Odors of the Enantiomeric Carvones. *J. Agric. Food Chem.* **1971**, *19* (4), 785–787.

(4) Bentley, R. *Reviews in Cell Biology and Molecular Medicine*; Meyers, R. A., Ed.; Wiley-VCH Verlag GmbH & Co. KGaA: Weinheim, Germany, 2006.

(5) Chhabra, N.; Aseri, M.; Padmanabhan, D. A Review of Drug Isomerism and Its

Significance. *Int. J. Appl. Basic Med. Res.* **2013**, *3* (1), 16.

(6) Maugh, T. H. Catalysts That Break Nature's Monopoly: Chiral Complexes Can Approach the Specificity of Enzymes for Synthesis of Optically Active Compounds, and Can Act on a Wider Variety of Substrates. *Science (80-.).* **1983**, *221* (4608), 351–354.

(7) Berova, N.; Nakanishi, K.; Woody, R. *Circular Dichroism: Principles and Applications*; John Wiley & Sons, 2000.

(8) Berova, N.; Polavarapu, P. L.; Nakanishi, K.; Woody, R. W. *Comprehensive Chiroptical Spectroscopy: Instrumentation, Methodologies, and Theoretical Simulations*; Wiley Online Library, 2012.

(9) Fasman, G. D. *Circular Dichroism and the Conformational Analysis of Biomolecules*; Springer Science & Business Media, 2013.

(10) Aćimović, S. S.; Ortega, M. a.; Sanz, V.; Berthelot, J.; Garcia-Cordero, J. L.; Renger, J.; Maerkl, S. J.; Kreuzer, M. P.; Quidant, R. LSPR Chip for Parallel, Rapid, and Sensitive Detection of Cancer Markers in Serum. *Nano Lett.* **2014**, *14* (5), 2636–2641.

(11) Yavas, O.; Svedendahl, M.; Dobosz, P.; Sanz, V.; Quidant, R. On-a-Chip Biosensing Based on All-Dielectric Nanoresonators. *Nano Lett.* **2017**, *17* (7), 4421–4426.

(12) Kabashin, a V; Evans, P.; Pastkovsky, S.; Hendren, W.; Wurtz, G. a; Atkinson, R.; Pollard, R.; Podolskiy, V. a; Zayats, a V. Plasmonic Nanorod Metamaterials for Biosensing. *Nat. Mater.* **2009**, *8* (11), 867–871.

(13) Svedendahl, M.; Verre, R.; Käll, M. Refractometric Biosensing Based on Optical Phase Flips in Sparse and Short-Range-Ordered Nanoplasmonic Layers. *Light Sci. Appl.* **2014**, *3* (11), e220.

(14) Kravets, V. G.; Schedin, F.; Jalil, R.; Britnell, L.; Gorbachev, R. V.; Ansell, D.; Thackray,

B.; Novoselov, K. S.; Geim, a. K.; Kabashin, a. V.; et al. Singular Phase Nano-Optics in Plasmonic Metamaterials for Label-Free Single-Molecule Detection. *Nat. Mater.* **2013**, *12* (2), 1–6.

(15) Zijlstra, P.; Paulo, P. M. R.; Orrit, M. Optical Detection of Single Non-Absorbing Molecules Using the Surface Plasmon Resonance of a Gold Nanorod. *Nat. Nanotechnol.* **2012**, *7* (6), 379–382.

(16) Chen, S.; Svedendahl, M.; Van Duyne, R. P.; Käll, M. Plasmon-Enhanced Colorimetric ELISA with Single Molecule Sensitivity. *Nano Lett.* **2011**, *11* (4), 1826–1830.

(17) Hentschel, M.; Schäferling, M.; Duan, X.; Giessen, H.; Liu, N. Chiral Plasmonics. *Sci. Adv.* **2017**, *3* (5), e1602735.

(18) Ogier, R.; Fang, Y.; Svedendahl, M.; Johansson, P.; Käll, M. Macroscopic Layers of Chiral Plasmonic Nanoparticle Oligomers from Colloidal Lithography. *ACS Photonics* **2014**, *1* (10), 1074–1081.

(19) Ogier, R.; Fang, Y.; Käll, M.; Svedendahl, M. Near-Complete Photon Spin Selectivity in a Metasurface of Anisotropic Plasmonic Antennas. *Phys. Rev. X* **2015**, *5* (4), 041019.

(20) Hentschel, M.; Schäferling, M.; Weiss, T.; Liu, N.; Giessen, H. Three-Dimensional Chiral Plasmonic Oligomers. *Nano Lett.* **2012**, *12* (5), 2542–2547.

(21) Verre, R.; Shao, L.; Odebo Länk, N.; Karpinski, P.; Yankovich, A. B.; Antosiewicz, T. J.; Olsson, E.; Käll, M. Metasurfaces and Colloidal Suspensions Composed of 3D Chiral Si Nanoresonators. *Adv. Mater.* **2017**, *29* (29), 1–6.

(22) Kuwata-Gonokami, M.; Saito, N.; Ino, Y.; Kauranen, M.; Jefimovs, K.; Vallius, T.; Turunen, J.; Svirko, Y. Giant Optical Activity in Quasi-Two-Dimensional Planar Nanostructures. *Phys. Rev. Lett.* **2005**, *95* (22), 227401.

(23) Schwanecke, A. S.; Krasavin, A.; Bagnall, D. M.; Potts, A.; Zayats, A. V; Zheludev, N. I. Broken Time Reversal of Light Interaction with Planar Chiral Nanostructures. *Phys. Rev. Lett.* **2003**, *91* (24), 247404.

(24) Yu, N.; Aieta, F.; Genevet, P.; Kats, M. a.; Gaburro, Z.; Capasso, F. A Broadband, Background-Free Quarter-Wave Plate Based on Plasmonic Metasurfaces. *Nano Lett.* **2012**, *12* (12), 6328–6333.

(25) Zhao, Y.; Belkin, M. A.; Alù, A. Twisted Optical Metamaterials for Planarized Ultrathin Broadband Circular Polarizers. *Nat. Commun.* **2012**, *3* (1), 870.

(26) Tang, Y.; Cohen, A. E. Enhanced Enantioselectivity in Excitation of Chiral Molecules by Superchiral Light. *Science (80-.).* **2011**, *332* (6027), 333–336.

(27) Tang, Y.; Cohen, A. E. Optical Chirality and Its Interaction with Matter. *Phys. Rev. Lett.* **2010**, *104* (16), 163901.

(28) Lipkin, D. M. Existence of a New Conservation Law in Electromagnetic Theory. *J. Math. Phys.* **1964**, *5* (5), 696–700.

(29) Meinzer, N.; Hendry, E.; Barnes, W. L. Probing the Chiral Nature of Electromagnetic Fields Surrounding Plasmonic Nanostructures. *Phys. Rev. B - Condens. Matter Mater. Phys.* **2013**, *88* (4), 1–5.

(30) Govorov, A. O.; Fan, Z.; Hernandez, P.; Slocik, J. M.; Naik, R. R. Theory of Circular Dichroism of Nanomaterials Comprising Chiral Molecules and Nanocrystals: Plasmon Enhancement, Dipole Interactions, and Dielectric Effects. *Nano Lett.* **2010**, *10* (4), 1374–1382.

(31) Maoz, B. M.; Chaikin, Y.; Tesler, A. B.; Bar Elli, O.; Fan, Z.; Govorov, A. O.; Markovich, G. Amplification of Chiroptical Activity of Chiral Biomolecules by Surface

Plasmons. *Nano Lett.* **2013**, *13* (3), 1203–1209.

(32) Lee, S.; Yoo, S.; Park, Q.-H. Microscopic Origin of Surface-Enhanced Circular Dichroism. *ACS Photonics* **2017**, *4* (8), 2047–2052.

(33) Schäferling, M.; Yin, X.; Giessen, H. Formation of Chiral Fields in a Symmetric Environment. *Opt. Express* **2012**, *20* (24), 26326–26336.

(34) Schäferling, M.; Dregely, D.; Hentschel, M.; Giessen, H. Tailoring Enhanced Optical Chirality: Design Principles for Chiral Plasmonic Nanostructures. *Phys. Rev. X* **2012**, *2* (3), 031010.

(35) García-Etxarri, A.; Dionne, J. a. Surface-Enhanced Circular Dichroism Spectroscopy Mediated by Nonchiral Nanoantennas. *Phys. Rev. B* **2013**, *87* (23), 235409.

(36) Ho, C.; Garcia-Etxarri, A.; Zhao, Y.; Dionne, J. Enhancing Enantioselective Absorption Using Dielectric Nanospheres. *ACS Photonics* **2017**, *4* (2), 197–203.

(37) Poulikakos, L. V.; Gutsche, P.; McPeak, K. M.; Burger, S.; Niegemann, J.; Hafner, C.; Norris, D. J. Optical Chirality Flux as a Useful Far-Field Probe of Chiral Near Fields. *ACS Photonics* **2016**, *3* (9), 1619–1625.

(38) Hendry, E.; Carpy, T.; Johnston, J.; Popland, M.; Mikhaylovskiy, R. V; Lapthorn, a J.; Kelly, S. M.; Barron, L. D.; Gadegaard, N.; Kadodwala, M. Ultrasensitive Detection and Characterization of Biomolecules Using Superchiral Fields. *Nat. Nanotechnol.* **2010**, *5* (11), 783–787.

(39) Zhao, Y.; Askarpour, A. N.; Sun, L.; Shi, J.; Li, X.; Alù, A. Chirality Detection of Enantiomers Using Twisted Optical Metamaterials. *Nat. Commun.* **2017**, *8*, 14180.

(40) Abdulrahman, N. a.; Fan, Z.; Tonooka, T.; Kelly, S. M.; Gadegaard, N.; Hendry, E.; Govorov, A. O.; Kadodwala, M. Induced Chirality through Electromagnetic Coupling

between Chiral Molecular Layers and Plasmonic Nanostructures. *Nano Lett.* **2012**, *12* (2), 977–983.

(41) Lu, F.; Tian, Y.; Liu, M.; Su, D.; Zhang, H.; Govorov, A. O.; Gang, O. Discrete Nanocubes as Plasmonic Reporters of Molecular Chirality. *Nano Lett.* **2013**, *13* (7), 3145–3151.

(42) Wang, R. Y.; Wang, P.; Liu, Y.; Zhao, W.; Zhai, D.; Hong, X.; Ji, Y.; Wu, X.; Wang, F.; Zhang, D.; et al. Experimental Observation of Giant Chiroptical Amplification of Small Chiral Molecules by Gold Nanosphere Clusters. *J. Phys. Chem. C* **2014**, *118* (18), 9690–9695.

(43) Schäferling, M. *Chiral Nanophotonics*; 2017.

(44) Klauk, H. *Organic Electronics: Materials, Manufacturing, and Applications*; John Wiley & Sons, 2006.

(45) Takahashi, J. I.; Shinojima, H.; Seyama, M.; Ueno, Y.; Kaneko, T.; Kobayashi, K.; Mita, H.; Adachi, M.; Hosaka, M.; Katoh, M. Chirality Emergence in Thin Solid Films of Amino Acids by Polarized Light from Synchrotron Radiation and Free Electron Laser. *Int. J. Mol. Sci.* **2009**, *10* (7), 3044–3064.

(46) Zarie, E. S.; Kaidas, V.; Gedamu, D.; Mishra, Y. K.; Adelung, R.; Furkert, F. H.; Scherließ, R.; Steckel, H.; Groessner-Schreiber, B. Solvent Free Fabrication of Micro and Nanostructured Drug Coatings by Thermal Evaporation for Controlled Release and Increased Effects. *PLoS One* **2012**, *7* (8).

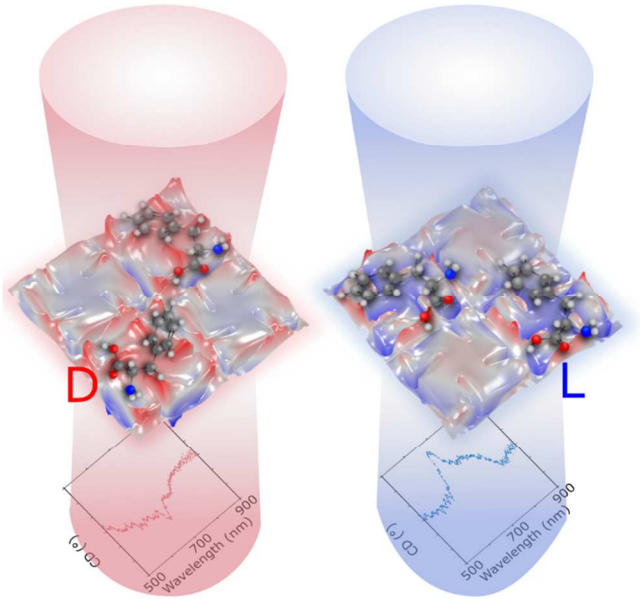

ToC Figure